Phase errors in high line density CGH used for aspheric testing: beyond scalar approximation

S. Peterhänsel*, C. Pruss and W. Osten

Institute of Applied Optics and Research Center SCoPE, University of Stuttgart, 70569 Stuttgart, Germany

*peterhaensel@ito.uni-stuttgart.de

Abstract: One common way to measure asphere and freeform surfaces is the interferometric Null test, where a computer generated hologram (CGH) is placed in the object path of the interferometer. If undetected phase errors are present in the CGH, the measurement will show systematic errors. Therefore the absolute phase of this element has to be known. This phase is often calculated using scalar diffraction theory. In this paper we discuss the limitations of this theory for the prediction of the absolute phase generated by different implementations of CGH. Furthermore, for regions where scalar approximation is no longer valid, rigorous simulations are performed to identify phase sensitive structure parameters and evaluate fabrication tolerances for typical gratings.

OCIS codes: (120.3180) Interferometry; (050.1970) Diffractive optics; (050.1755) Computational electromagnetic methods.

References and links

1. J. C. Wyant and V. P. Bennett, "Using Computer Generated Holograms to Test Aspheric Wavefronts," Appl. Opt. **11** 2833–2839 (1972).
2. S. M. Arnold, "How to test an asphere with a computer-generated hologram," Proc. SPIE **1052** 191–197 (1989).
3. E.-B. Kley, W. Rockstroh, H. Schmidt, A. Drauschke, F. Wyrowski, and L.-C. Wittig, "Investigation of large null-CGH realization," Proc. SPIE **4440** (2001).
4. J. Ma, C. Pruss, M. Häfner, B. Heitkamp, R. Zhu, Z. Gao, C. Yuan, and W. Osten, "Systematic analysis of the measurement of cone angles using high line density computer-generated holograms," Opt. Eng. **50** (2011).
5. S. Reichelt, C. Pruss, and H. J. Tiziani, "Specification and characterization of CGHs for interferometrical optical testing," Proc. SPIE **4778** (2002).
6. Y.-C. Chang, P. Zhou, and J. H. Burge, "Analysis of phase sensitivity for binary computer-generated holograms," Appl. Opt. **45** 4223–4234 (2006).
7. P. Zhou and J. H. Burge, "Fabrication error analysis and experimental demonstration for computer-generated holograms," Appl. Opt. **46** 657–663 (2007).
8. P. Lalanne and D. Lemercier-Lalanne, "On the effective medium theory of subwavelength periodic structures," J. Mod. Opt. **43** 2063–2085 (1996).
9. W. Yu, K. Takahara, T. Konishi, T. Yotsuya, and Y. Ichioka, "Fabrication of Multilevel Phase Computer-Generated Hologram Elements Based on Effective Medium Theory," Appl. Opt. **39** 3531–3536 (2000).
10. I. Richter, P.-C. Sun, F. Xu, and Yeshayahu Fainman, "Design considerations of form birefringent microstructures," Appl. Opt. **34** 2421–2429 (1995).
11. N. Bokor, R. Shechter, N. Davidson, A. A. Friesem, and Erez Hasman "Achromatic Phase Retarder by Slanted Illumination of a Dielectric Grating with Period Comparable with the Wavelength," Appl. Opt. **40** 2076–2080 (2001).
12. W. Iff, S. Glaubrecht, N. Lindlein, and J. Schwider, "Untersuchung der Abweichungen zwischen skalarer und rigoroser Rechnung an CGHs in Twyman-Green-Interferometern zur Linsenprüfung," DGaO-Proceedings http://www.dgao-proceedings.de (2010).

13. J. D. Gaskill, *Linear Systems, Fourier Transforms and Optics,* (Wiley, 1978).
14. Y. Sheng, D. Feng, and S. Larochelle, "Analysis and synthesis of circular diffractive lens with local linear grating model and rigorous coupled-wave theory," J. Opt. Soc. Am. A **14** 1562–1568 (1997).
15. M. Totzeck, "Numerical simulation of high-NA quantitative polarization microscopy and corresponding near-fields," Optik - International Journal for Light and Electron Optics **112** (2001).
16. L. Li and Gérard Granet, "Field singularities at lossless metal-dielectric right-angle edges and their ramifications to the numerical modeling of gratings," J. Opt. Soc. Am. A **28** 738–746 (2011).
17. L.Li, " Field singularities at lossless metaldielectric arbitrary-angle edges and their ramifications to the numerical modeling of gratings," J. Opt. Soc. Am. A **29** 593-604 (2012).
18. E. D. Palik, *Handbook of optical constants of solids,* (Academic Press, 1991).
19. J. Turunen and F. Wyrowski, *Diffractive optics for industrial and commercial applications,* (Akademie Verlag, 1997).
20. E. Popov, M. Nevière, B. Gralak, and G. Tayeb, "Staircase approximation validity for arbitrary-shaped gratings," J. Opt. Soc. Am. A **19** (2002).
21. P. Zhou and J. H. Burge, "Optimal design of computer-generated holograms to minimize sensitivity to fabrication errors" Opt. Express **15** 15410–15417 (2007).

1. Introduction

The trend in optics towards more complex, lighter and smaller optical systems has pushed the demand for steep aspheres and freeform surfaces. This also pushes the demand for fast and accurate testing of these surfaces. One method for testing is the well known Null-Test [1,2] shown in Fig. 1. Here a CGH placed in the object path of an interferometer generates a wavefront that matches the surface under test, resulting in an interferogram that shows no fringes for a perfect test surface. If wavefront distortions are measured, they can be attributed to fabrication errors of the test surface. However this only holds true, if the CGH itself has no or only known defects, as errors of the CGH will also be present in the interferogram and induce a systematic error in the test setup. Hence, one needs to control or calibrate the errors induced by fabrication tolerances of the CGH. As the trend in optics design goes towards steeper aspheres the grating periods of

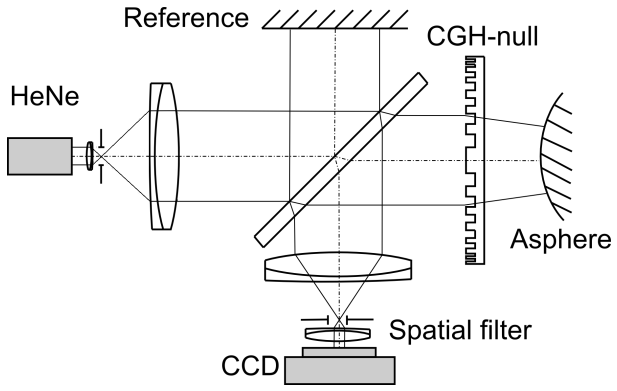

Fig. 1: Null test for an asphere: A CGH is placed in the object path to generate a wavefront that matches the asphere. Fabrication errors of the asphere can be determined, if the effects of the interferometer itself and the CGH are known.

the CGH are getting smaller. At the same time, actual fabrication technologies allow to produce CGH with high fringe densities, so it is tempting for the designer to use these capabilities [3,4]. Most of the CGHs are designed using scalar approximation. Influences by fabrication errors were studied using a scalar model [5–7] or the effective media approach [8, 9]. However, if CGHs with periods of only a few or below the wavelength of the reconstructing light are used,

the influence of rigorous effects might cause a non tolerable deviation between designed and reconstructed phase. In addition the influence of the polarisation state of the incident light has to be considered. The different behaviour of the generated phase for TE and TM polarised light is used in the design of phase retarders [10, 11]. However, for those applications the phase difference for TE and TM polarised light is of importance, whereas for the Null test the absolute phase generated by the grating is key. Therefore when using gratings in the rigorous regime the polarisation of the light has to be taken into account to know the generated phase.

Previous work in the field of rigorous modelling of CGHs has been done by e.g. *Kley et al.* [3] and *Iff et al.* [12].

In this paper we will focus on the phase error caused by structure parameter variations for CGHs for small periods and compare the scalar approximation to rigorous results. For the rigorous simulations the RCWA is used.

In section 2 limits of the scalar approximation are discussed for binary gratings. Section 3 shows the phase changes induced by fabrication errors in the CGH production for binary gratings. A second type of grating, blazed gratings, is analysed in section 4. All results will be summarised in section 5.

2. Limitations of Scalar Diffraction Theory

For a comparison with the scalar approximation, we first consider a binary grating. Using the Fraunhofer diffraction theory for a normal incident plane wavefront on to a grating with period Λ, line width b, duty cycle $D = b/\Lambda$ and height h, the complex amplitude of the far field wavefront function U can be written as shown in Eq. 1 [6, 13]. Here A_0 and A_1 correspond to the output wavefront amplitude from the top and the bottom of the grating.

$$U = \begin{cases} A_0 + [A_1\cos(\xi) - A_0]D + iA_1\sin(\xi)D & m = 0 \\ [A_1\cos(\xi) - A_0]D\mathrm{sinc}(mD) + iA_1\sin(\xi)D\mathrm{sinc}(mD) & m = \pm 1, \pm 2\ldots \end{cases} \tag{1}$$

Where ξ is defined as:

$$\xi = \frac{(n-1)d}{\lambda} \cdot 2\pi \tag{2}$$

Using Eq. 1 the phase function ϕ is defined by the ratio of imaginary and real part of U and can be written as:

$$\tan\phi = \frac{\Im\{U\}}{\Re\{U\}} = \begin{cases} \frac{A_1\sin(\xi)D}{A_0 + [A_1\cos(\xi) - A_0]D} & m = 0 \\ \frac{A_1\sin(\xi)\mathrm{sinc}(mD)}{[A_1\cos(\xi) - A_0]\mathrm{sinc}(mD)} & m = \pm 1, \pm 2\ldots \end{cases} \tag{3}$$

The output phase ϕ is given in radians. For simplicity we will use the wavefront phase W which is defined as:

$$W = \frac{\phi}{2\pi} \tag{4}$$

To determine the limit of the scalar approximation, binary phase gratings in reflection with decreasing periods were simulated using RCWA. The wavefront phase was compared to the scalar values for the 1$^{\mathrm{st}}$ order ($m = 1$), as this order is most used for interferometry. For the scalar approximation an ideal reflection was assumed ($A_0 = A_1 = 1$).

Figure 2(a) shows the result for a grating with a duty cycle D of 0.5 and a structure height corresponding to a phase change W of 0.5. Another interesting point is duty cycle sensitivity. Scalar theory states that the phase of the first order is independent from the duty cycle of the grating; not so the results from the rigorous simulations, see Fig. 2(b).

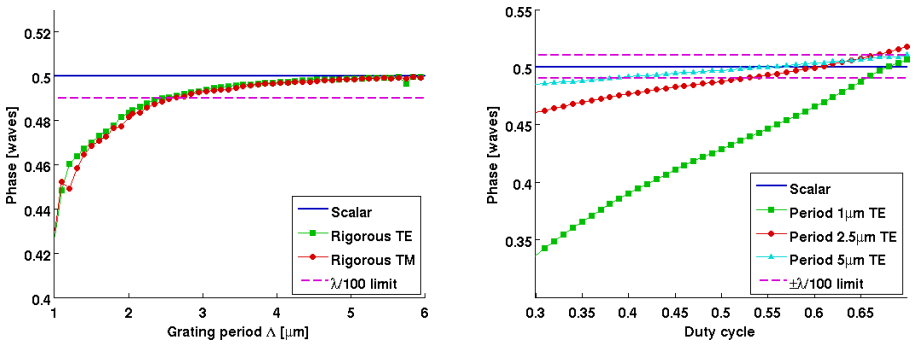

(a) Variable grating period

(b) Variable duty cycle

Fig. 2: Comparison of scalar approximation and rigorous simulation for (a) binary grating with duty cycle of 0.5 and variable grating period and (b) variable duty cycle for different grating periods. Illumination wavelength is set to 633 nm.

In both figures a limit of $\lambda/100$ was introduced to give a more practical estimation of the induced error when using scalar approximation. For a fixed duty cycle of 0.5, i.e. without any tolerance assumptions, a common choice for CGH in interferometry, the limit was reached for periods of 2.6 – 2.8 µm for a wavelength of 633 nm. As the change in the refractive index for glass in the region of the visible light is smooth, one might estimate more generally, that a phase error of $\lambda/100$ is already reached for structures with 4λ period. As for structures with changing D, as seen in Fig. 2(b), even for structures with a period of 5 µm the $\lambda/100$ limit can be reached, although this requires a rather drastic change in the duty cycle (values smaller than 0.37 or values larger than 0.7). For smaller periods the range, where an error smaller than $\lambda/100$ is induced, is decreasing rapidly. The summary of this section is that even for moderate line densities, one needs to use rigorous methods, when producing structures with high requirements (e.g. when only phase errors smaller than $\lambda/100$ are allowed).

3. Sensitivity analysis: Binary gratings

In this section, we investigate the effects of structure parameter variations onto the phase reconstructed by a null-CGH. We restrict our considerations to binary linear gratings, as null-CGH can be well approximated with a locally periodic line grating (LGA) [14]. Since also the aperture under which the CGHs are used is getting larger, the simulations were executed with a conical illumination covering angles of incident light up to a NA of 0.5. The used illumination wavelength was set to 633 nm. To determine the effect of small variations of the desired structure parameters, the phase differences were calculated for a perfect grating and a grating with variations of 1 % in one parameter. The studied parameters are: the line width (b), height, side wall angle (α) for transmission plus thickness of the Cr-layer (d) for reflection. The start values for the gratings are: Height $h = 694$ nm, Side wall angle $\alpha = 88°$, thickness of the Cr-layer of $d = 80$ nm. As periods $\Lambda_1 = 1$ and $\Lambda_2 = 2$ µm were chosen with a duty cycle of 0.5 resulting in line widths of $b_1 = 0.5$ and $b_2 = 1$ µm. A sketch of the simulated structures can be found in Fig. 3. All simulations were done using the ITO inhousetool MicroSim [15].

First a test for the convergence behaviour for both gratings has to be done, as convergence problems are present for certain types of gratings when using RCWA [16, 17]. Therefore the efficiency η of the 1st order was studied over the truncation order M. This was done for perpendicular and angluar (30°) incident light, see Fig. 4. For both gratings the truncation order was

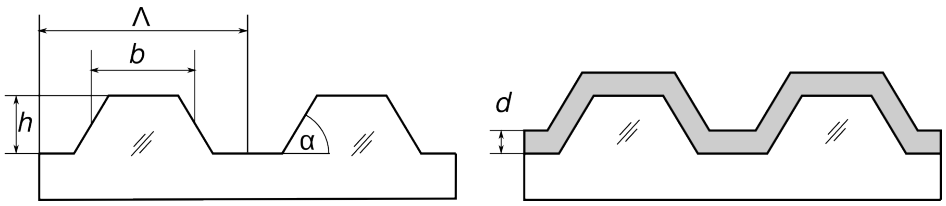

(a) Transmission grating (b) Reflection grating

Fig. 3: Models of the simulated gratings for use in transmission and reflection.

set to $M = 50$.

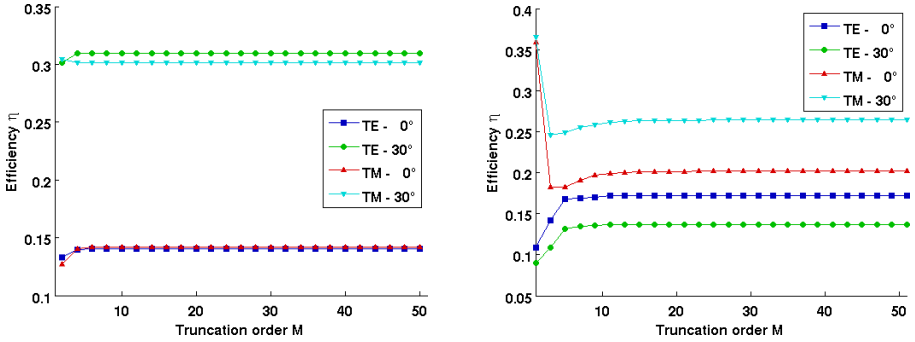

(a) Transmission grating (b) Reflection grating

Fig. 4: Convergence check of the used binary gratings: Both types of gratins show a quick convergence, even for slanted illumination. The truncation order M was set to 50.

As we focus on phase errors due to rigorous effects only, a scalar calculation was also done for the same parameter variations. The studied phase error ΔW is then given by the difference between the rigorous calculated and the scalar phase change:

$$\Delta W = \Delta W_{\text{rig}} - \Delta W_{\text{scalar}} \tag{5}$$

ΔW describes the pure rigorous effects that are neglected in a scalar treatment like polarisation effects and effects due to the angle of incidence.

3.1. Transmission gratings

To evaluate the dependence of the phase from the variations in the structure geometry, the 0^{th} and $\pm 1^{\text{st}}$ order were simulated. In Fig. 5 the resulting phase difference ΔW for the binary grating in transmission are shown for both grating periods. The difference was plotted using contours with a separation of $\lambda/100$.

For the binary grating the following result was observed: For all parameters essentially the same behaviour was found for TE and TM polarisation, therefore only one polarisation is shown in Fig. 5. As for variations in b, the difference for the $+1^{\text{st}}$ order between rigorous and scalar calculation are reduced from $\lambda/40$ to nearly zero when the period Λ is increased from 1 to 2 µm. For the 0^{th} order the difference stays almost the same. For variations in height phase differences

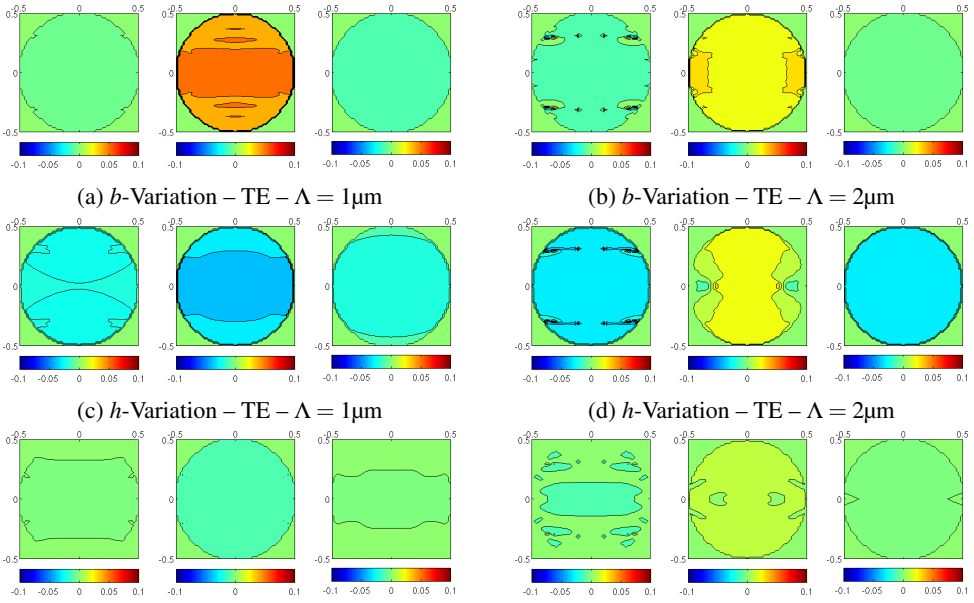

(a) b-Variation – TE – $\Lambda = 1\mu$m (b) b-Variation – TE – $\Lambda = 2\mu$m

(c) h-Variation – TE – $\Lambda = 1\mu$m (d) h-Variation – TE – $\Lambda = 2\mu$m

(e) α-Variation – TE – $\Lambda = 1\mu$m (f) α-Variation – TE – $\Lambda = 2\mu$m

Fig. 5: Changes in phase for line gratings used in transmission for linewidth, height and sidewall variations of 1 % using TE polarised light. Column 1 shows the +1st order, column 2 shows the 0th order and column 3 shows the -1st order.

of up to $\lambda/20$ can be seen for all orders and all angles of incidence. The phase shows nearly no sensitivity regarding α, hence the differences between scalar and rigorous calculation can be neglected for sidewall angles close to 90°. Results for TM polarisation can be found in appendix A. For periods of 2 µm ($\lambda = 633$ nm) one can observe some angles of incidence in the 1st order where the phase difference is quite large. This behaviour is due to phase jumps in this region.

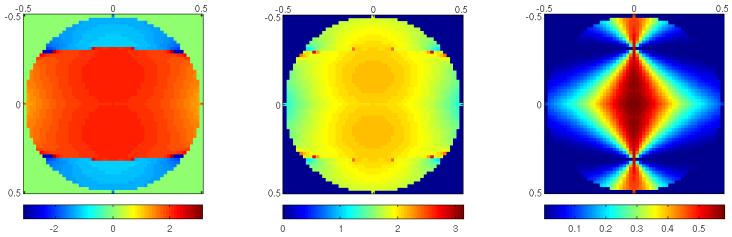

(a) Phase ϕ – TE (b) Unwrapped phase ϕ – TE (c) Intensity – TE

Fig. 6: Angular phase dependence of the 1st order for a structure with period of 2 µm: (a) output phase, (b) phase after unwrapping and (c) Intensity distribution for the given structure.

For the evaluation of the phase, unwrapping was done (see Fig. 6). However, there are some regions remaining where the phase is not changing smoothly as one would expect. When looking at the corresponding intensity distribution one finds that in these regions next to no intensity

can be measured. To conclude: The high phase differences for certain angles are due to phase jumps and due to the fact that they are present in regions of very low intensity can be treated as numerical artefacts.

3.2. Reflection grating

In interferometry, apart from transmissive phase structures also reflective CGH are required, e.g. for alignment structures or as calibration elements for transmissive systems. A typical implementation is depicted in Fig. 3(b). The CGH has a metal layer (e.g. Cr) on top of the fused silica structure in order to increase the reflection. For this type of grating the same analysis for effects on the phase caused by fabrication errors as for the transmission binary grating was done.

In Fig. 7 the changes in phase can be seen for variations in b and α for gratings with periods of 1 and 1.5 µm. As the metal layer shows a strong effect on the polarisation, both polarisation directions are shown. Results for height and thickness of the Cr-layer are shown in appendix C. The optical properties of the chromium used in the simulations are: $n = 3.136$ and $k = 3.312$ (for $\lambda = 633$ nm). In addition the same calculations have been done using the different n- and k values from *Palik* [18] ($n = 3.5763$, $k = 4.3615$ for $\lambda = 633$ nm). No apparent change in the results was observed.

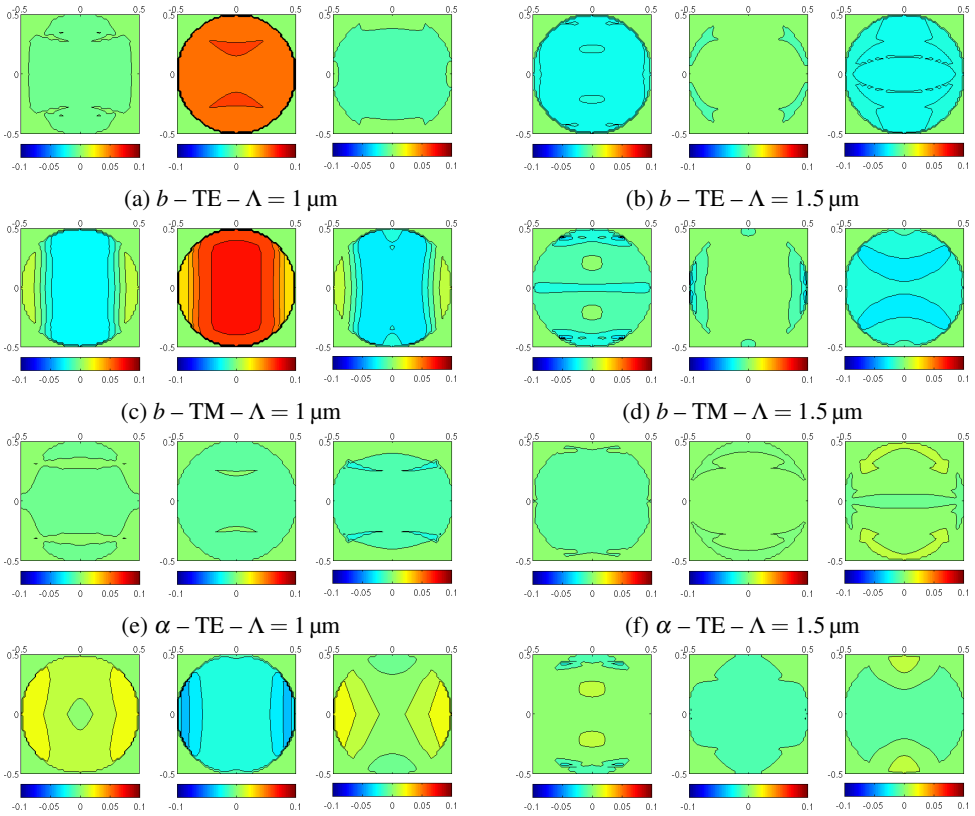

(a) b – TE – $\Lambda = 1$ µm (b) b – TE – $\Lambda = 1.5$ µm

(c) b – TM – $\Lambda = 1$ µm (d) b – TM – $\Lambda = 1.5$ µm

(e) α – TE – $\Lambda = 1$ µm (f) α – TE – $\Lambda = 1.5$ µm

(g) α – TM – $\Lambda = 1$ µm (h) α – TM – $\Lambda = 1.5$ µm

Fig. 7: Simulation results for the phase change caused by 1% parameter variation for a binary grating with a Cr-layer used in reflection.

In contrast to the results for the purely dielectric gratings in transmission, a very strong dependence on the polarisation is observed. The generated phase changes are much larger for TM polarised light than for TE. In addition the dependence of the incidence angle is quite strong as the phase change for b variations for the $\pm 1^{\text{st}}$ order varied from $-\lambda/30$ for perpendicular incidence to $+\lambda/50$ for oblique incident light (30°). Also changes in the α show a strong effect on the phase, whereas for gratings in transmission nearly no effect was seen. In addition the changes between scalar and rigorous calculations are varying significantly when the period is increased from 1 to 1.5 µm, as gratings with $\Lambda = 1.5\,\mu\text{m}$ show next to no dependence on the polarisation.

4. Sensitivity analysis: Blazed transmission gratings

A second important structure used for CGHs are blazed gratings, shown in Fig. 8(a). The same comparison between scalar and rigorous calculation was done as for binary gratings (see section 2). The studied structure is a blazed grating used in transmission made of fused silica with a phase change of 2π and periods from 1 to 4 µm. Figure 8(b) shows the increasing deviation between rigorous and scalar calculated phase. For structure sizes smaller than 3 µm the induced error is larger than $\lambda/100$.

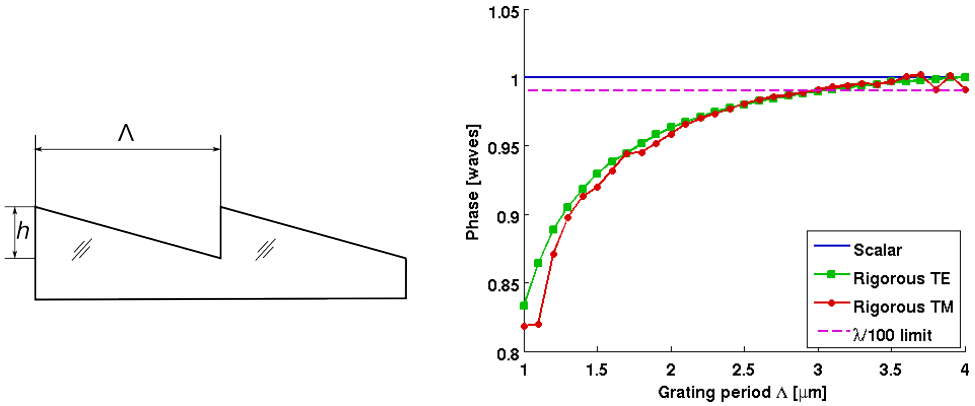

(a) (b)

Fig. 8: (a) Model of the blazed transmission grating used in the calculations
(b) Comparison between scalar and rigorous simulation for the generated phase of a blazed grating. For small structure sizes the difference between scalar and rigorous are increasing rapidly.

Also a sensitivity analysis is done for structures with periods of 1 and 2 µm. Here variations of 1% in height are studied for blazed gratings. The phase changes are shown in Fig. 9, please note that the range of the used scale has increased from ± 0.1 to ± 0.2. As for the binary gratings, the $\pm 1^{\text{st}}$ and 0^{th} order are shown. The difference in the phase change between rigorous and scalar calculations has values of $\lambda/20$ up to $\lambda/10$. These values are approximately the same for both periods. As both polarisations show quite similar results, the TE polarisation can be found in appendix B.

For the production of blazed CGH two methods are commonly used: binary multilevel fabrication and the grey scale process. Both will be studied here. A more general description of these processes and others can be found in [19].

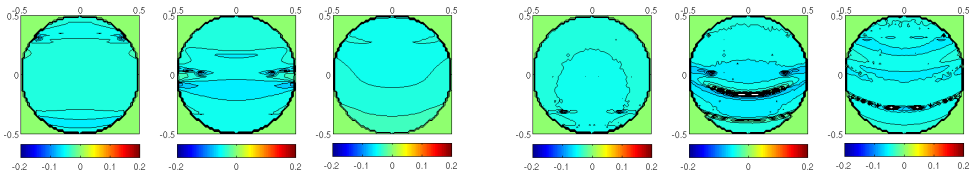

(a) h – TM – $\Lambda = 1\,\mu$m (b) h – TM – $\Lambda = 2\,\mu$m

Fig. 9: Calculated phase changes for 1 % parameter change of a blazed grating with a height of 1.39 µm.

4.1. Multilevel binary gratings

The advantage of this method is the efficiency of the well known binary lithography process. The resulting structures of this method are staircase approximations of the intended grating. The challenge of this method is the correct alignment of the masks, especially for gratings with small periods. The influence of the misalignment Δx on the phase was investigated for a 4-layer system, produced by a two-mask-process. Gratings with periods from 1 to 4 µm were analysed. The misalignment was varied in the range of $\Delta x = p \cdot 0.1$. Examples of the modelled structures are shown in Fig. 10.

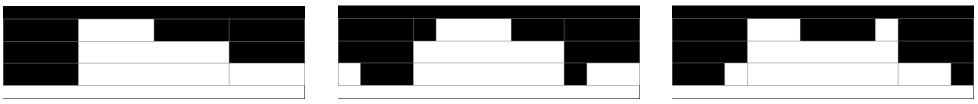

(a) $\Delta x = 0\,$nm (b) $\Delta x = +75\,$nm (c) $\Delta x = -75\,$nm

Fig. 10: Binary blaze structure with a period of 1 µm and a misalignment Δx of 0 and ± 75 nm.

To get a better understanding how one would expect the phase to change due to misalignment, a comparison to the scalar calculation was done. Figure 11 shows the generated phase for scalar and rigorous calculations for perpendicular incident light. One can observe that for larger period sizes the difference between TE and TM polarised light gets smaller and the overall difference compared to the scalar calculation also decreases.

The simulations, see Fig. 12, show the dependence of the generated phase for different angles of incidence for the used 1st order. It can be seen that the generated phase along the whole range of the observed angles varies strongly. Also even small misalignments cause a great deviation from the predicted phase. This might be expected, as for small Δx isolated structures occur, which have a strong effect on the generated phase.

4.2. Grey scale process

Another common way to produce blazed diffractive structures is laser or e-beam direct writing in a grey scale process. Here the intensity of the laser is changed during the writing process to generate the change in height of the structure e.g. with the help of a low contrast photo resist process. This will lead to a smooth blazed grating but due to the finite writing spot also to edge rounding. To evaluate how round edges affect the generated phase, gratings with increasing edge rounding were simulated. The rounding was described by the width σ of the Gaussian function we use as an approximation of our writing spot profile. For a continuously scanning writing spot, the resulting intensity pattern can be described as a convolution between perfect grating profile and spot profile, see Eq 6 where $*$ denotes the convolution operator.

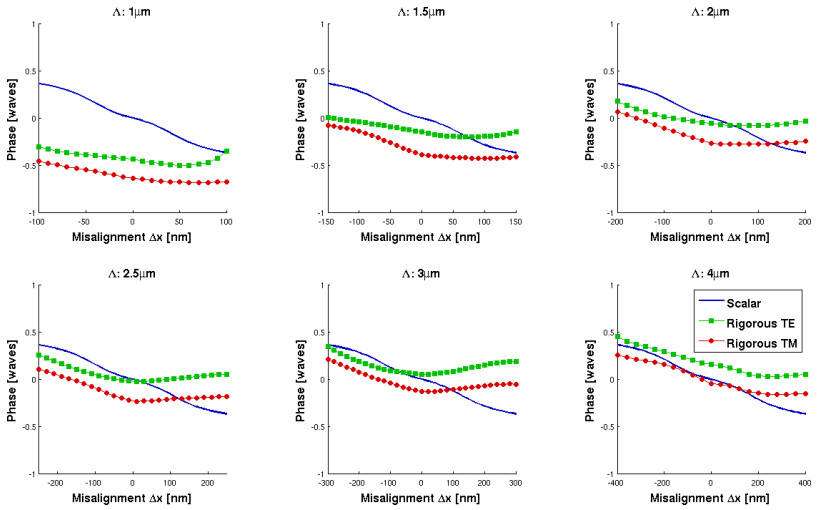

Fig. 11: Comparison of scalar and rigorous calculations of the phase for misaligned masks and perpendicular incident light.

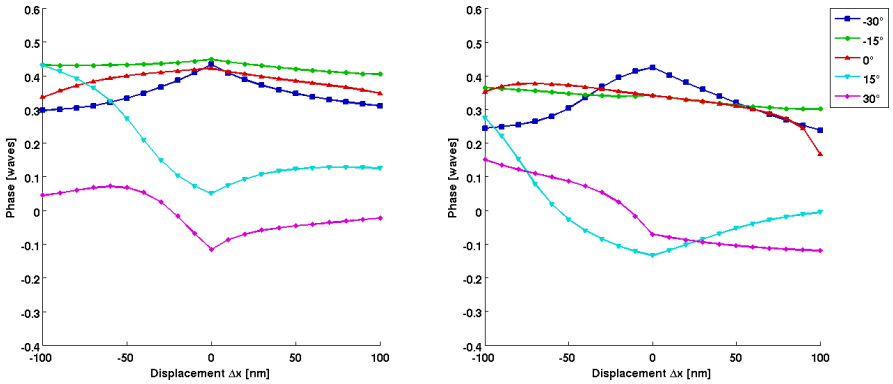

(a) TE polarisation

(b) TM polarisation

Fig. 12: Dependence of the generated phase over misalignment Δx for grating period $\Lambda = 1\,\mu\text{m}$: It can be seen that even for a small misalignment the resulting change in phase can not be neglected. There is also a strong dependence of the phase on the angle of incidence.

$$g_{\text{round}}(x) = g(x) * \frac{1}{\sqrt{2\pi}\sigma} \exp\left(-\frac{x^2}{2\sigma^2}\right) \tag{6}$$

The width σ of the Gaussian function was varied between 5 and 100 nm and the effect on the generated phase was observed for oblique and perpendicular incident light. Figure 13 shows the resulting structure for a 1 μm period grating with σ set to 50 nm.

Due to using RCWA the structure is approximated by a staircase approach, which effects the results in the near field, but has no effect in the studied far field, if enough layers are used [20]. The dependence of the number of used layers on the generated phase has been studied and the

Fig. 13: Modelled structure with edge rounding. For the calculations 78 layers were used, resulting in a height of 17.79 nm for each layer.

results for both polarisations can be found in Fig 14.

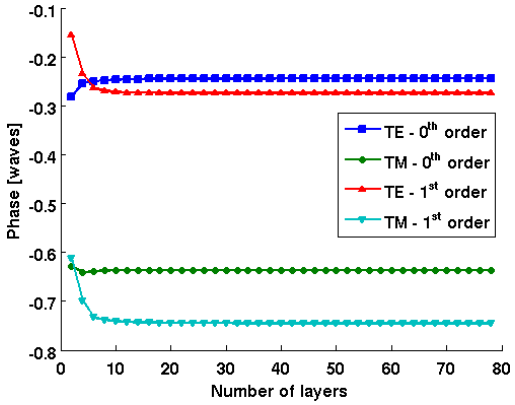

Fig. 14: Dependence of generated phase over the number of used layers for RCWA simulation.

In Fig. 15 the behaviour of the phase change ΔW for 1% variation in height over sigma are shown.

For periods of 1 µm the induced phase difference is quite constant over the increasing edge rounding. Also both rigorous and scalar simulation show the same general behaviour althoug the difference in the phase change is about 0.15 waves. The differences between TE and TM polarisation are much smaller in comparison but increase if the illumination angle is increased.

5. Conclusion and Outlook

Computer generated holograms are a powerful tool in asphere and freeform testing. However, they constitute an important part of the error budget of the testing procedure, especially since their calibration is not trivial. Fabrication tolerances have been taken into account to find optimal designs of the CGHs micro structures [21]. In this contribution we have addressed the influence of electromagnetic effects that cannot be described with scalar approximation. Even a perfect fused silica CGH deviates more than $\lambda/100$ from what would be expected in scalar approximation, if the local grating periods are smaller than 4.5 λ for a wavelength of 633 nm. This is true for binary and blazed structures. In addition to that, fabrication tolerances introduce additional phase errors. To identify structure parameters, that have a significant effect on the generated phase, rigorous sensitivity analysis have been done for typical gratings. A variation of 1 % was introduced for selected parameters. The following results were found for grating periods of 1 µm at 633 nm wavelength.

For binary gratings in transmission variations in height showed the largest difference be-

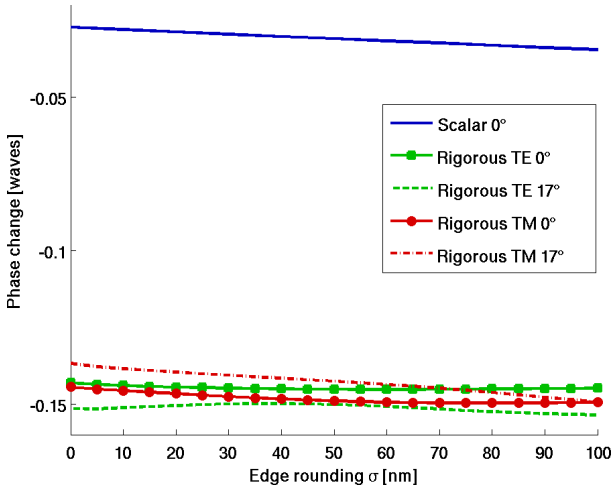

Fig. 15: Change of induced phase change by small parameter variation over increasing edge rounding. The rigorous simulations were done for perpendicular incident light and 17° oblique incident light. For a comparison scalar results are also shown for perpendicular incident light.

tween scalar and rigorous calculation with deviations up to $\lambda/20$. Phase changes in line width b showed values of $\lambda/30$ for TE polarisation. If metallised CGH are used in reflection with TM polarised light, phase changes of up to $\lambda/10$ were observed for changes in b. Also the side wall angle α caused changes of up to $\lambda/30$. Increasing the period to 1.5µm typically decrease the phase changes for most parameters significantly as well as the dependence on polarisation.

Blazed gratings showed a large dependence of the height, creating phase changes of up to $\lambda/10$ again for a variation of 1 %. Fabrication methods for blazed gratings as grey scale and multi-level binary process show strong dependence of incident angle and the alignment of the separate layers for multilevel process. Especially for small structures with period sizes of 1 µm, there are heavy constraints if the allowed phase error is in the regime of $\lambda/100$. Since usual fabrication tolerances generate phase errors well above $\lambda/100$, a calibration method to characterise the phase of the CGH has to be found. As next step the problem of finding easy accessible parameters that correspond to the change in phase will be addressed. Therefore the inverse problem between intensities of ellipsometric measurements and the related phase needs to be studied and evaluated by measurements.

A. Binary grating in transmission

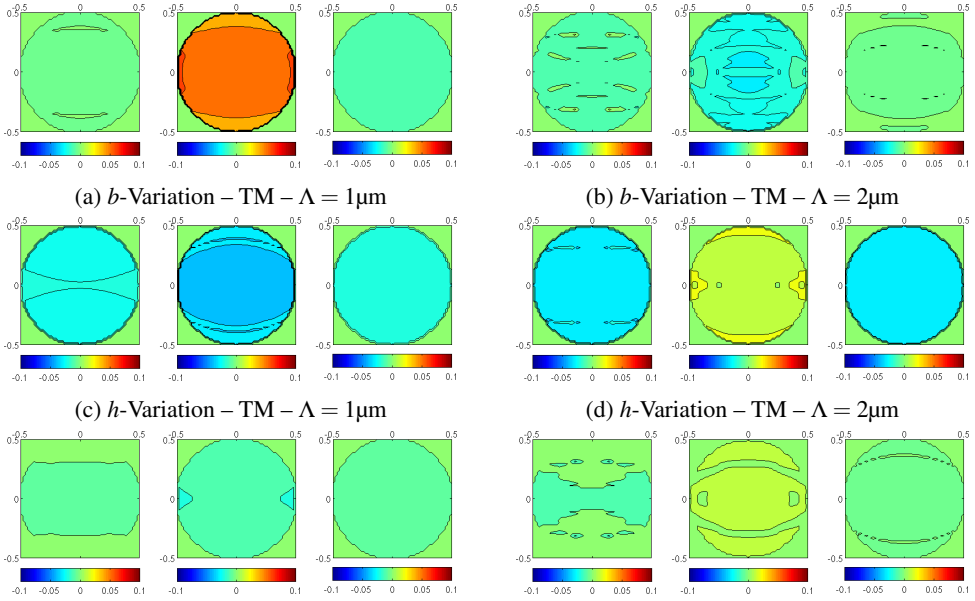

(a) b-Variation – TM – $\Lambda = 1\mu m$ (b) b-Variation – TM – $\Lambda = 2\mu m$

(c) h-Variation – TM – $\Lambda = 1\mu m$ (d) h-Variation – TM – $\Lambda = 2\mu m$

(e) α-Variation – TM – $\Lambda = 1\mu m$ (f) α-Variation – TM – $\Lambda = 2\mu m$

Fig. 16: Changes in phase for line gratings used in transmission for line width, height and side wall variations of 1 % using TM polarised light.

B. Blazed grating

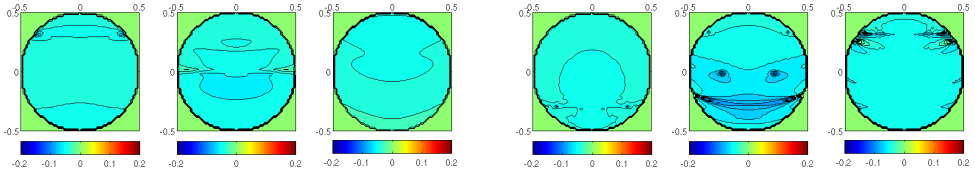

(a) h – TE – $\Lambda = 1\mu m$ (b) h – TE – $\Lambda = 2\mu m$

Fig. 17: Calculated phase changes for 1 % parameter change of a blazed grating with pitch of 1 µm and height of 1.39 µm.

C. Binary grating in reflection

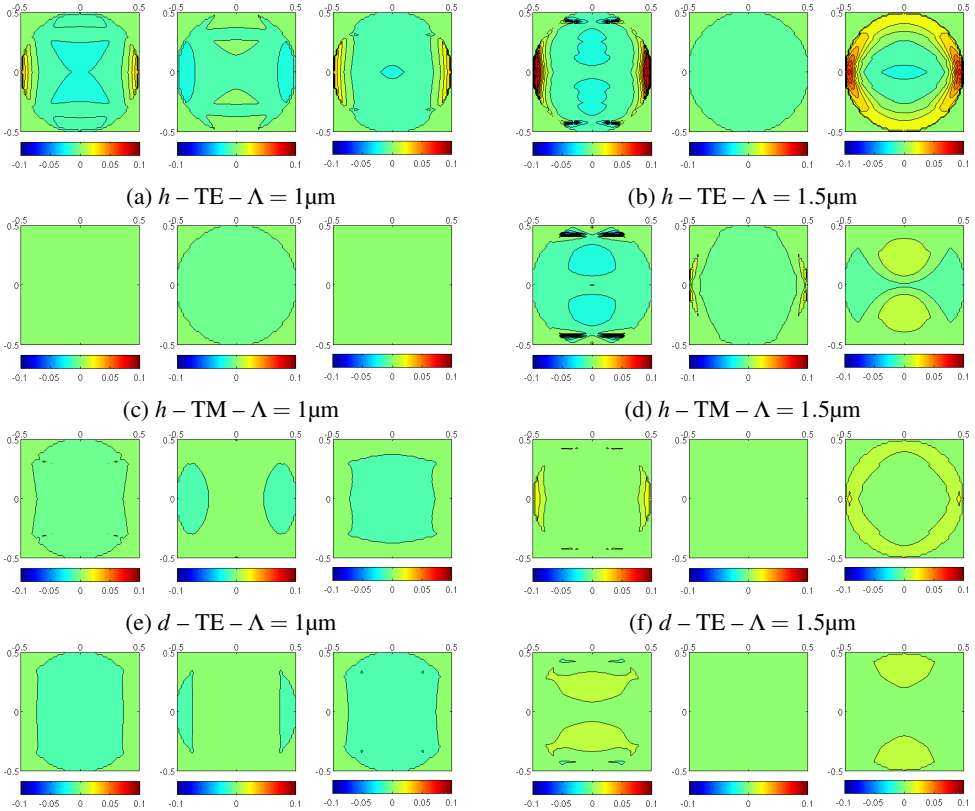

(a) h – TE – $\Lambda = 1\mu m$ (b) h – TE – $\Lambda = 1.5\mu m$

(c) h – TM – $\Lambda = 1\mu m$ (d) h – TM – $\Lambda = 1.5\mu m$

(e) d – TE – $\Lambda = 1\mu m$ (f) d – TE – $\Lambda = 1.5\mu m$

(g) d – TM – $\Lambda = 1\mu m$ (h) d – TM – $\Lambda = 1.5\mu m$

Fig. 18: Simulation results for the phase change caused by 1% parameter variation for a binary grating with a Cr-layer used in reflection.

Acknowledgements

This work was supported by the German Research Foundation (DFG) in the scope of the project "Inverse source and inverse diffraction problems in photonics" (OS111/32-1) and within the DFG funding programme Open Access Publishing.